Article

Combinatorial Approach toward High-Throughput Analysis of Direct Methanol Fuel Cells

Rongzhong Jiang, Charles Rong, and Deryn Chu

J. Comb. Chem., **2005**, 7 (2), 272-278• DOI: 10.1021/cc0498581 • Publication Date (Web): 06 January 2005

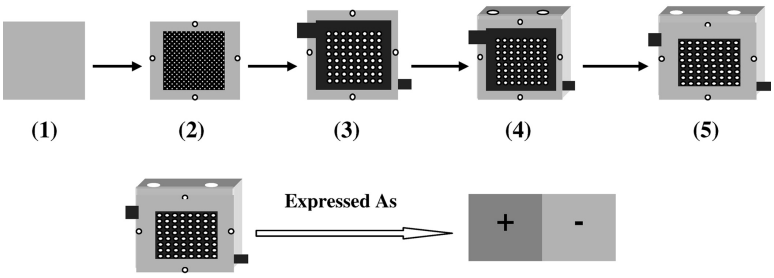

More About This Article

Additional resources and features associated with this article are available within the HTML version:

- Supporting Information
- Links to the 2 articles that cite this article, as of the time of this article download
- Access to high resolution figures
- Links to articles and content related to this article
- Copyright permission to reproduce figures and/or text from this article

View the Full Text HTML

Journal of Combinatorial Chemistry is published by the American Chemical Society.
1155 Sixteenth Street N.W., Washington, DC 20036

Combinatorial Approach toward High-Throughput Analysis of Direct Methanol Fuel Cells

Rongzhong Jiang,* Charles Rong, and Deryn Chu

U.S. Army Research Laboratory, 2800 Powder Mill Road, Adelphi, Maryland 20783-1197

Received September 7, 2004

A 40-member array of direct methanol fuel cells (with stationary fuel and convective air supplies) was generated by electrically connecting the fuel cells in series. High-throughput analysis of these fuel cells was realized by fast screening of voltages between the two terminals of a fuel cell at constant current discharge. A large number of voltage−current curves (200) were obtained by screening the voltages through multiple small-current steps. Gaussian distribution was used to statistically analyze the large number of experimental data. The standard deviation (σ) of voltages of these fuel cells increased linearly with discharge current. The voltage−current curves at various fuel concentrations were simulated with an empirical equation of voltage versus current and a linear equation of σ versus current. The simulated voltage−current curves fitted the experimental data well. With increasing methanol concentration from 0.5 to 4.0 M, the Tafel slope of the voltage−current curves (at $\sigma = 0.0$), changed from 28 to 91 mV·dec^{-1}, the cell resistance from 2.91 to 0.18 Ω, and the power output from 3 to 18 mW·cm^{-2}.

Introduction

Fuel cell is considered to be one of the most promising technologies for energy generation, which directly converts hydrogen and air into electricity and produces water with zero emission. Recently, the research and development of fuel cells has received much attention.[1−11] Generally, fuel cell development requires doing large amounts of electrochemical measurements, such as the study of catalysts, electrodes, electrolytes, bipolar plates, and membrane electrode assemblies (MEAs). To solve the problem of time-consuming measurements, a combinatorial approach was proposed by Reddington and coauthors[12] for seeking new electrocatalysts in 1998. The combinatorial method originated from biological analysis, but its wide applications in material science began only in the middle of the 1990s when Xiang and coauthors introduced it to the study of high-temperature superconductors.[13] Currently, the combinatorial method has become a powerful tool for high-throughput synthesis and characterization of advanced materials.[14−21]

Since the pioneering work of Reddington and coauthors for combinatorial methods in electrochemistry, several research articles[22−27] have been published with a variety of methods for generating electrode arrays and development of screening methods, that is, optical screening,[12] automated screening,[22] and electrolyte−probe screening.[27] The application of combinatorial methods in fuel cell research[28−33] has mainly focused on catalysts and electrode-reactions. So far, there are few reports on the generation of fuel cell arrays or libraries in which each member in the array is a complete single fuel cell. The present paper describes a high-throughput screening method for analysis of a fuel cell array by direct voltage measurements and data treatment with a statistical method. In a practical fuel cell system, dozens or hundreds of single fuel cells are combined together to achieve higher voltage, current, and power. Such a combination of fuel cells is called a fuel cell stack. However, if there is one "poor" single cell in the fuel cell, the performance of the whole fuel cell stack will be greatly reduced. It is important for the fuel cell manufacturers to analyze the performance of all the single fuel cells before they are assembled as fuel cell stacks. The combinatorial method provides a fast, efficient, and accurate way to analyze a large number of single fuel cells, fuel cell arrays, or fuel cell libraries.

Experimental Section

Chemicals and Materials. Nafion 117 membrane was purchased from DuPont Chemical Company. Before being used for fuel cell preparation, it was chemically treated by two steps. The first step was 3% H_2O_2 treatment at 80 °C for 2 h, and then being washed to remove the residue H_2O_2. The second step was 2 M H_2SO_4 treatment at a boiling condition for 2 h, and being washed again to remove the residue acid. The fuel cell grade Pt black (for cathode catalyst) and PtRu black (for anode catalyst) were purchased from Johnson Matthey Company. Titanium sheets (0.7 mm thick) were used for anode and cathode current collectors. E-Tek's one-sided carbon cloth was used as the gas and fuel diffusion layers, which were placed between the electrode and the current collector in the single cell.

Single Cell Processing. The membrane electrode assemblies (MEAs) were made by hot-pressing the Pt black (loading 5 mg·cm^{-2}), Nafion 117 membrane, and the PtRu black (loading of 5 mg·cm^{-2}) together (5% Nafion solution was used as the binder for the catalyst powders). The active electrode area was 9 cm^2. A single direct methanol fuel cell

* To whom correspondence should be addressed. Phone: 301-394-0295. Fax: 301-394-0273. E-mail: RJiang@Arl.Army.mil.

10.1021/cc0498581 CCC: $30.25
Published on Web 01/06/2005

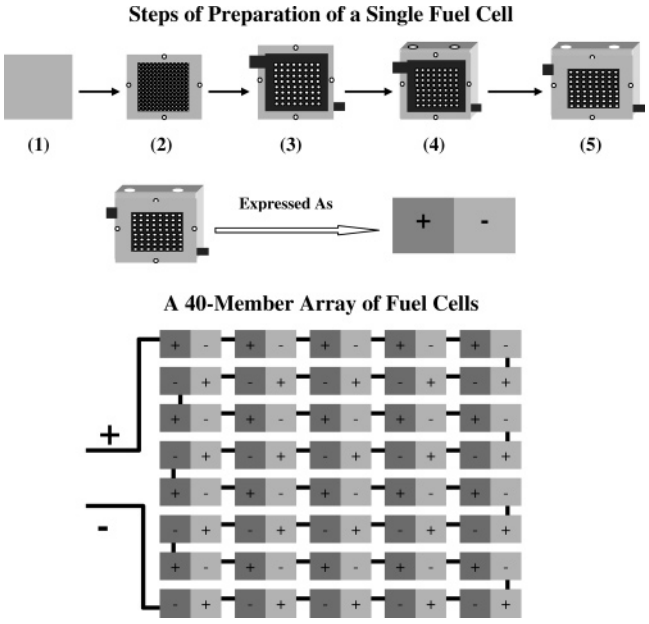

Figure 1. Schematic view of the steps of preparation of a single fuel cell (upper panel), and a fuel cell array (lower panel) containing 40 single fuel cells that are generated by electrically connecting individual single fuel cells in series for combinatorial measurements at constant current discharge. Steps of preparation of a single fuel cell: (1) start from a polymer electrolyte membrane, (2) attach catalysts to the membrane, (3) attach current collectors, (4) attach fuel compartment and anode end-plate, and (5) attach cathode end-plate.

(DMFC) was constructed by assembling a series of parts together in the order of end plate, current collector, carbon cloth, MEA, carbon cloth, current collector, methanol compartment, and end plate. A schematic view of a complete single DMFC assembly is shown in the upper panel in Figure 1. In the present experiment, 0.5−4.0 M methanol was used as fuel and the ambient air as oxidant. The air was supplied to the fuel cell by spontaneous convection, and the fuel was supplied by diffusion from a stationary methanol compartment.

Fuel Cell Array. A fuel cell array with 40 single fuel cells was generated by electrical connection of a number of fuel cells in series, as shown in the lower panel in Figure 1.

Instrumentation. An electronic load (model no. 6050A) and a multimeter from Hewlett-Packard were used to measure the single cell's current and voltage, respectively. All experiments were carried out at room temperature (25 °C).

Results and Discussion

Fuel Cell Array and Screening Method. Figure 1 shows a method of generating a fuel cell array. There are 40 single fuel cells that use stationary methanol as fuel and ambient air as oxidant by spontaneous convection. A 40-member array was formed by electrical connection of these fuel cells in series, one cell's negative terminal linked to another's positive terminal. The fuel cell array was characterized electrochemically under constant current discharge. Here, every single fuel cell in the array had the same current but different voltages. Therefore, the performance of any of the individual fuel cells was determined by measuring the voltages of that fuel cell. A high-throughput screening was realized by measuring the voltage between the negative and the positive terminals of each single fuel cell with two electric probes linked with a multimeter. The voltage of a fuel cell in the array was obtained instantly. The screenings of 40 fuel cells were completed in only a few minutes for one discharge current. Since all of these fuel cells were measured under the same conditions (i.e., the same current and temperature) and these measurements were finished in a short period of time, the experimental accuracy was improved significantly.

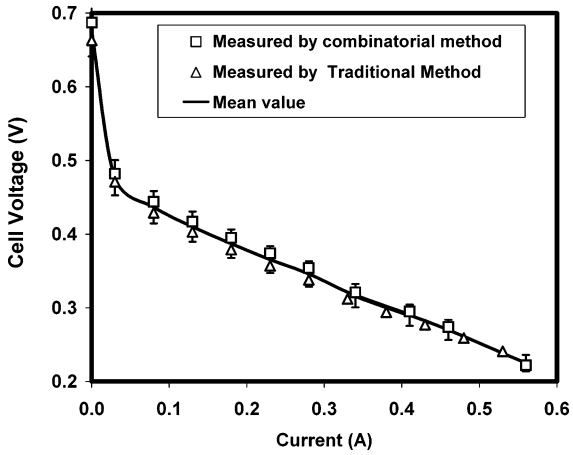

Figure 2. Voltage−current curve of DMFC obtained by single cell alone (outside the array) and by the combinatorial method (inside the array). Fuel: 2.0 M methanol. Electrode area: 9 cm^2. The solid line is obtained by averaging the data of single cell and combinatorial measurements. Error bar: 5%.

Voltage−Current Curve of a Single Fuel Cell. A single fuel cell's voltage−current curve was obtained by changing the discharge current from low to high and measuring the cell voltage at each current. The voltage response at zero discharge current (i.e., open circuit condition) was unstable due to the methanol crossover[34,35] through the electrolyte membrane from the anode to the cathode. However, once a very low current (i.e., 0.03 A or more) was drawn from the fuel cell, the voltage responded quickly, and the electrochemical reactions in the fuel cell reached equilibrium in a few seconds because the catalysts on the electrodes were activated and the influence of methanol crossover on the discharge voltage was limited. Figure 2 shows a voltage−current curve of a single fuel cell, where the points were obtained by combinatorial screening of one single fuel cell in the array and a traditional linear potential scan of a single fuel cell outside of the array, respectively. The line in the figure was obtained by averaging the data from the combinatorial and traditional methods. These experimental points by the two different methods have a deviation of 5%, which implies that the results from the combinatorial method is consistent with that of the traditional method.

Voltage−Current Curves of A 40-Member Fuel Cell Array. Figure 3 shows voltage current curves of a 40-member fuel cell array for methanol concentrations from 0.5 to 4.0 M. There are 40 experimental curves for each methanol concentration, or 200 curves for the total of the five methanol concentrations, which were obtained by multiple steps of constant current discharge and measuring the voltages of each cell. The total number of data points acquired was ∼2000.

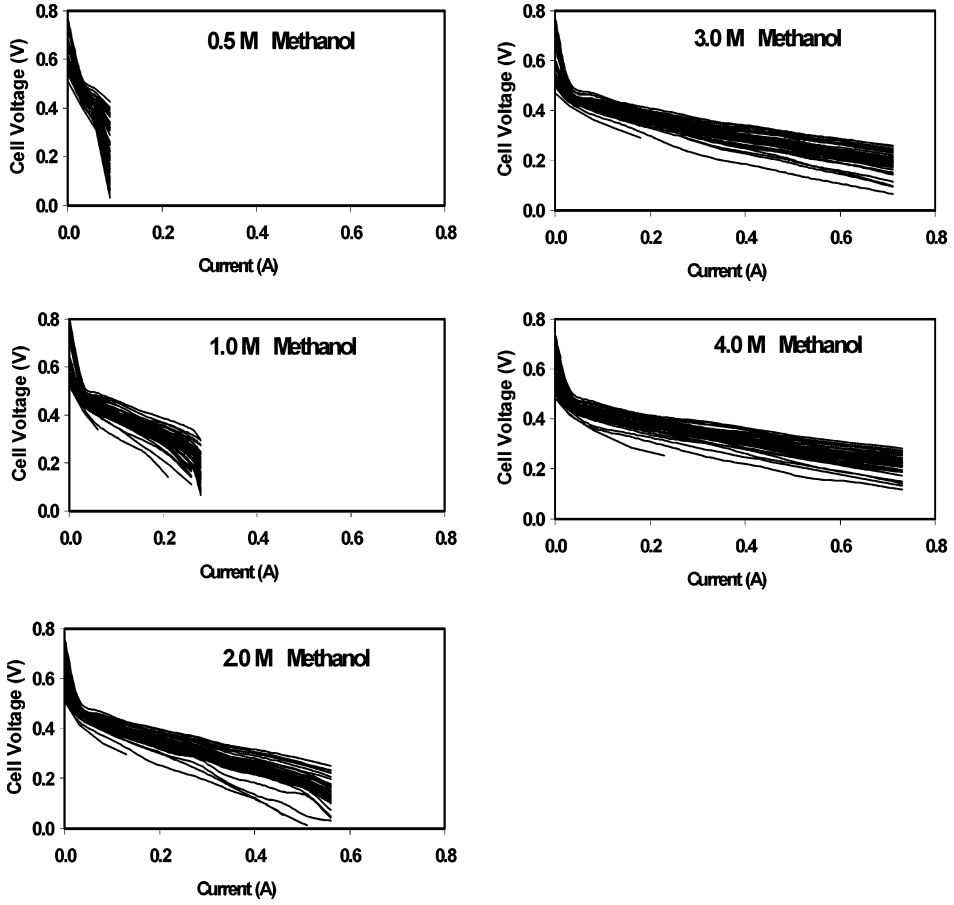

Figure 3. Voltage−current curves of a 40-member DMFC array with various fuel concentrations at room temperature (25 °C). Electrode area: 9 cm^2.

The total experiments for screening of voltage were completed in only a few hours. However, if the traditional electrochemical method was used by linear potential scan, it would take more than 10 days to complete the same number of experiments.

Each of the voltage−current curves contains a complete description of an individual single fuel cell's performance under a specific experimental condition (such as fuel concentration). As the better performing fuel cells have the higher voltage at the same discharge current, the voltage−current curves of the better fuel cells are shown in the upper region in these figures. Apparently, these voltage−current curves of single fuel cells are distributed in a wide voltage range because of significant performance differences. On the other hand, with increasing methanol concentration, the performance of these single fuel cells is improved appreciably. The higher methanol concentration gives rise to the higher discharge voltage at the same discharge current. The average discharge current at 0.2 V for 4.0 M methanol concentration is significantly raised to around 700 mA, which is ∼7 times more than that for the 0.5 M methanol concentration.

Statistical Analysis. To more clearly and logically analyze the large number of experimental voltage−current curves shown in Figure 3, a statistical method was employed. Since all of these single fuel cells were made in the same way, for example, the same catalysts (loading of 5 $mg \cdot cm^{-2}$), electrolyte membrane, electrode area, current collector, and fuel concentration, the voltage data obtained from the 40 single fuel cells under constant current discharge would obey statistical laws. Following are the statistical analysis and mathematical simulation of these voltage−current curves.

(1) Gaussian Distribution and Standard Deviation. One set of voltage screening from the combinatorial measurements of the fuel cell array generated 40 voltage data points under one discharge current. The 40 voltage data points can be statistically treated with a Gaussian distribution, which is given by

$$F(\nu) = \frac{1}{\sigma\sqrt{2\pi}} e^{-(\nu-\mu)/2\sigma^2} \quad (1)$$

Here, $F(\nu)$ is Gaussian distribution function of voltage; σ (V) is the standard deviation from a group of measurements; μ (V) is the mean value, or the average of voltages for these measurements; and ν (V) is the individual value of voltages.

Figure 4 shows the Gaussian distributions of 12 groups of voltage data obtained at 12 steps of constant current discharge for a methanol concentration of 3.0 M, where each group of voltages corresponds to one discharge current. At zero discharge current (or open circuit condition), the Gaussian distribution curve covers a wide range with an abnormally high standard deviation due to the instability of open circuit voltage. Therefore, the zero current condition will not be used for mathematical simulation. All the other curves in Figure 4 show a typical standard Gaussian distribution. For each of the curves, a large number of the experimental data points are distributed around the mean

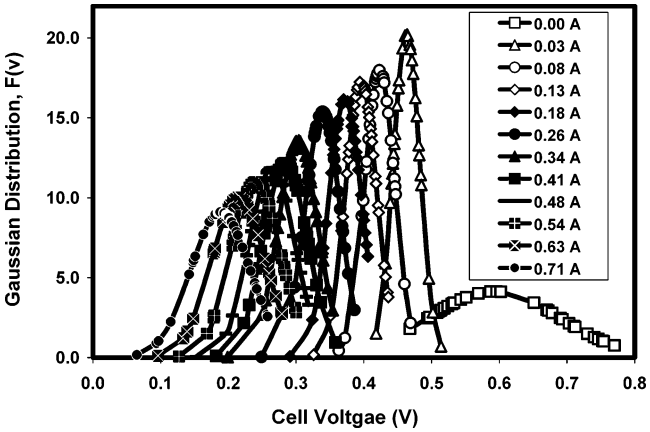

Figure 4. Gaussian distribution of fuel cells' voltages for a 40-member DMFC array at constant current discharge. Fuel: 3.0 M methanol.

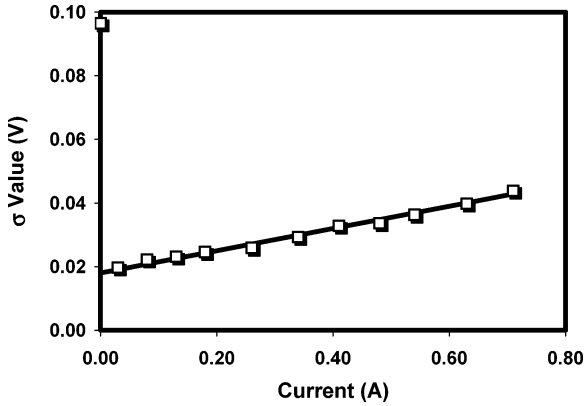

Figure 5. Standard deviation of fuel cells' voltages versus discharge current for a 40-member DMFC array. Fuel: 3.0 M methanol.

value, and only a few of them are located on the left and right sides far from the peak (mean) of the Gaussian distribution. Interestingly, the mean value of voltages decreases and the Gaussian distribution becomes wider with the increasing the discharge current. This implies that higher discharge current results in larger standard deviation of voltage. Figure 5 shows the plot of standard deviation of voltage versus discharge current. The standard deviations can be described by a linear equation, with an exception of the point for the open circuit condition, which is given by

$$\sigma = \sigma_0 + Si \tag{2}$$

Here, σ_0 (V) is the ideal standard deviation at zero current, which is obtained by extrapolating the linear line to zero current as shown in Figure 5; S (V·A^{-1}) is the slope of σ versus discharge current; and i (A) is the discharge current.

(2) Empirical Equation. The voltage−current curve can be described with an empirical equation[36,37] which is given by

$$E_i = E_0 - b \log(1000i) - Ri \tag{3}$$

Here, E_i (V) is an individual fuel cell's voltage at any discharge current; E_0 (V) is the voltage at zero discharge current; b (V·dec^{-1}) is the Tafel slope of the voltage−current curve; and R (Ω) is the resistance of the fuel cell.

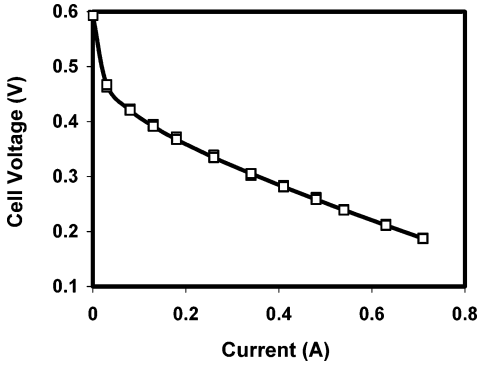

Figure 6. Voltage−current curves obtained from the mean values of voltages for a 40-member DMFC array at constant current discharge. Fuel: 3.0 M methanol. The points are the experimental mean values, and the solid line is obtained by calculation with eq 3.

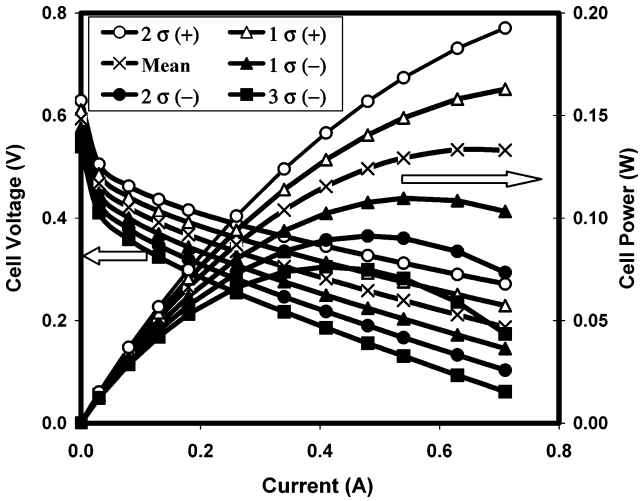

Figure 7. Calculated voltage−current and power−current curves between $+2.0\sigma$ and -3.0σ for a 40-member DMFC array. Fuel: 3.0 M methanol. The σ and mean values are obtained from the statistical treatment of the experimental data.

Figure 6 shows a voltage−current curve obtained from the mean values of the voltages for a 40-member fuel cell array using 3.0 M methanol as fuel. The points are experimental data, and the line is the calculated curve using the eq 3. As expected, the calculated curve is in good agreement with the experimental points.

(3) Simulation of Electrochemical Behavior of Fuel Cell Array. Combining eqs 2 and 3, we can mathematically simulate the voltage−current curves of the fuel cell array in Figure 3. Figure 7 shows a series of calculated voltage−current and power−current curves with various standard deviations from -3σ to $+2\sigma$ for the 40-member fuel cell array using 3.0 M methanol as fuel. The simulated voltage−current curves for standard deviations from -3σ to $+2\sigma$ in Figure 7 fit well with the 40 experimental voltage−current curves shown in Figure 3 for 3.0 M methanol. In another words, we can describe the electrochemical behavior of the fuel cell array by only two equations if we know the electrochemical parameters listed in Tables 1 and 2.

The successful simulation of the voltage−current curves of the fuel cell array for 3.0 M methanol has encouraged us to treat the data of the fuel cell array for other fuel concentrations.

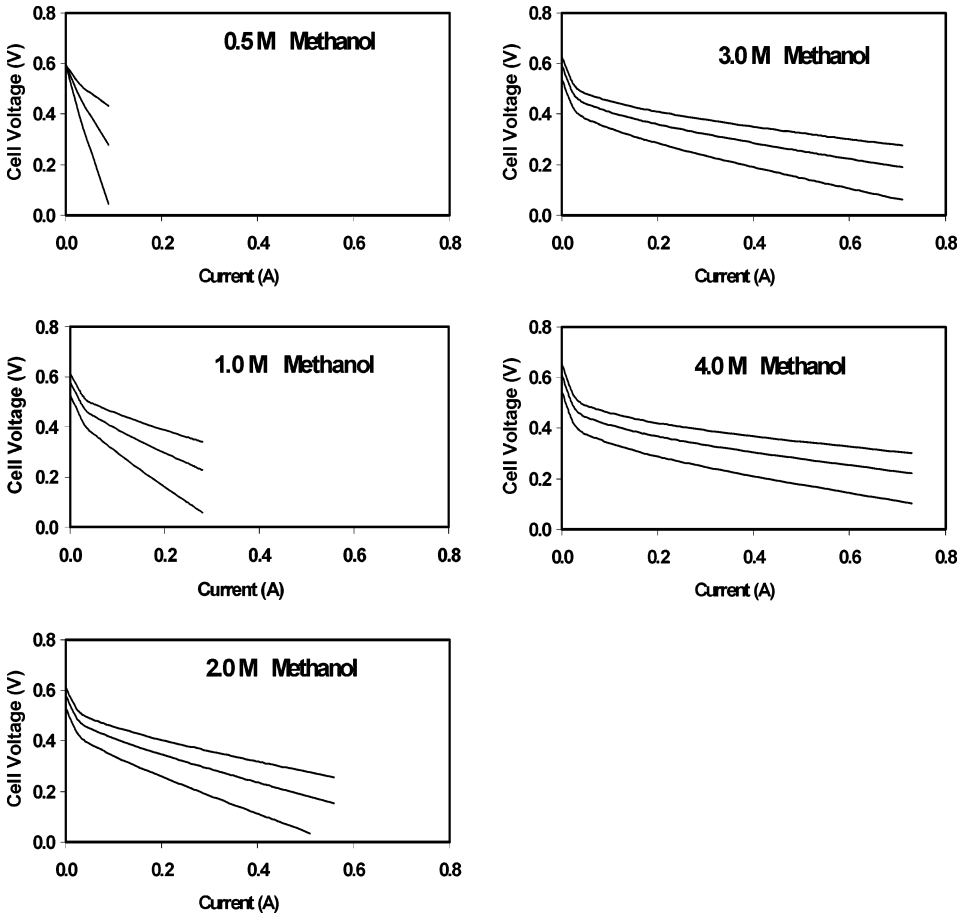

Figure 8. Calculated voltage−current curves between $+2\sigma$ and -3σ for a 40-member DMFC array with various fuel concentrations. Electrode area: 9 cm^2.

Table 1. Parameters Used for Calculations of the Mean Values of Voltage−Current Curves for a 40-Member DMFC Array[a]

methanol (mol·L^{-1})	E_0 (V)	b (V·dec^{-1})	R (Ω)
4.0	0.612	0.091	0.177
3.0	0.593	0.080	0.247
2.0	0.578	0.061	0.459
1.0	0.580	0.057	0.760
0.5	0.594	0.028	2.910

[a] Equation: $E_i = E_0 - b \log(1000i) - Ri$.

Table 2. Parameters Used for Calculation of the Standard Deviation for a 40-Member DMFC Array[a]

methanol (mol·L^{-1})	σ_0 (V)	S (V·A^{-1})
4.0	0.0215	0.0248
3.0	0.0180	0.0350
2.0	0.0160	0.0606
1.0	0.0170	0.1410
0.5	0.000	0.8630

[a] Equation: $\sigma = \sigma_0 + Si$.

Figure 8 shows the calculated voltage−current curves between standard deviations -3σ and $+2\sigma$ by eqs 2 and 3 for the 40-member fuel cell array for methanol concentrations from 0.5 to 4.0 M. All of these voltage−current curves fit the experimental data of Figure 3 well. Table 1 summarizes the electrochemical parameters used for the calculations of the mean values of the fuel cell array. With increasing methanol concentration from 0.5 to 4.0 M, the E_0 values show no appreciable change, but the Tafel slope (b value) of the voltage−current curve increases from 28 to 91 mV·dec^{-1}, and the R value decreases from 2.91 to 0.18 Ω. The increase of the Tafel slope of the voltage−current curve indicates a lower kinetic rate for catalytic oxygen reduction due to the contamination of the cathode catalyst by methanol crossover. The decrease of the R value results from less resistance of fuel diffusion because of higher methanol concentration. Table 2 lists the values of σ_0 and S that are used for the calculation of σ values for methanol concentrations from 0.5 to 4.0 M. With increasing methanol concentration, the σ_0 increases only slightly, but the S value decreases significantly.

Table 3. Maximum Single Cell Power at Various σ Values for the 40-Member DMFC Array Obtained within Experimental Current Range[a]

methanol (mol·L^{-1})	maximum single cell's power (W)					
	-3σ	-2σ	-1σ	0σ	$+1\sigma$	$+2\sigma$
4.0	0.0882	0.1080	0.1333	0.1622	0.1911	0.2200
3.0	0.0761	0.0914	0.1102	0.1346	0.1650	0.1954
2.0	0.0555	0.0654	0.0782	0.0945	0.1156	0.1429
1.0	0.0343	0.0409	0.0507	0.0636	0.0776	0.0915
0.5	0.0129	0.0160	0.0191	0.0250	0.0320	0.0389

[a] Electrode area: 9 cm^2.

Figure 9 shows the calculated power-current curves of the 40 member fuel cell array using the data in Figure 8 for methanol concentrations from 0.5 to 4.0 M. The performance of these single fuel cells in the fuel cell array is summarized in Table 3. With increasing methanol concentration from 0.5

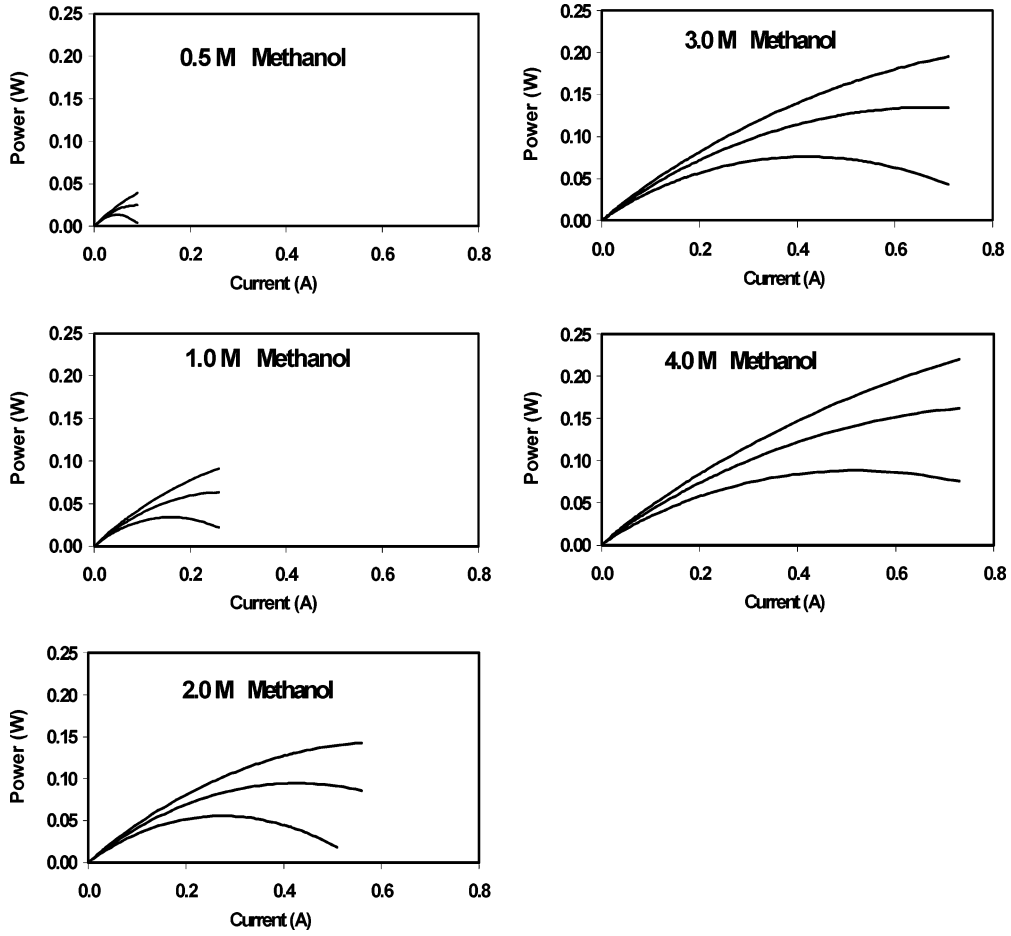

Figure 9. Calculated power−current curves between $+2\sigma$ and -3σ for a 40-member DMFC array with various fuel concentrations. Electrode area: 9 cm^2.

to 4.0 M, the power output increases significantly. For 4.0 M methanol concentration, the best single fuel cell has a power output of 220 mW (or 24 $mW\cdot cm^{-2}$), and the worst has 88 mW (or 10 $mW\cdot cm^{-2}$), respectively. The majority of the power outputs of the single fuel cells (i.e., those around the mean value of the power output) is 162 mW (or 18 $mW\cdot cm^{-2}$).

Conclusion

A 40-member array of fuel cells was generated by a series of electrical connections of single fuel cells. A high-throughput screening of voltages was realized by simple electric contacting of the positive and negative terminals of each of the single fuel cells using two conductive probes. The voltage−current curve obtained by the combinatorial method was in good agreement with that obtained by traditional linear potential scans with 5% deviation. The large numbers of experimental data at various methanol concentrations were statistically analyzed with a Gaussian distribution. The experimental voltage−current curves were simulated with an empirical equation of voltage versus current and a linear equation of standard deviation versus current. The calculated voltage−current curves between -3σ and $+2\sigma$ matched well with the experimental results. With increasing methanol concentration, the Tafel slope (b value) of the voltage−current curve increases from 28 to 91 $mV\cdot dec^{-1}$ due to methanol crossover, and the R value decreases from 2.91 to 0.18 Ω due to less resistance of fuel diffusion at high methanol concentration. The power output increases significantly with increasing methanol concentration. At 4.0 M methanol concentration, the power outputs are 10 $mW\cdot cm^{-2}$ for -3σ, 16 $mW\cdot cm^{-2}$ for 0.0σ, and 24 $mW\cdot cm^{-2}$ for $+2\sigma$. The differences in the performance of the fuel cells can be attributed to a small difference of actual catalyst loading[27] on the electrodes by experimental deviation.

Acknowledgment. The authors thank the U.S. Department of the Army and the Army Materiel Command for their financial support.

References and Notes

(1) Appleby, A. J. *Energy* **1996**, *21*, 521−652.
(2) Carrette, L.; Friedrich, K. A.; Stimming, U. *ChemPhysChem* **2000**, *1*, 162−193.
(3) Acres, G. J. K. *J. Power Sources* **2001**, *100*, 60−66.
(4) Mehta, V.; Cooper, J. S. *J. Power Sources* **2003**, *114*, 32−53.
(5) Bernay, C.; Marchand, M.; Cassir, M. *J. Power Sources* **2002**, *108*, 139−152.
(6) Tuber, K.; Zobel, M.; Schmidt, H.; Hebling, C. *J. Power Sources* **2003**, *122*, 1−8.
(7) Wasmus, S.; Kuver, A. *J. Electroanal. Chem*. **1999**, *461*, 14−31.
(8) Jiang, R. Z.; Chu, D. *J. Power Sources* **2001**, *93*, 25−31.
(9) Surampudi, S.; Narayanan, S. R.; Vamos, E.; Frank, H.; Halpert, G.; Laconti, A.; Kosek, J.; Prakash, G. K. S.; Olah, G. A. *J. Power Sources* **1994**, *47*, 377−385.

(10) Ren, X. M.; Wilson, M. S.; Gottesfeld, S. *J. Electrochem. Soc*. **1996**, *143*, L12-L15.
(11) Fan, Q. B.; Pu, C.; Smotkin, E. S. *J. Electrochem. Soc*. **1996**, *143*, 3053−3057.
(12) Reddington, E.; Sapienza, A.; Gurau, B.; Viswanathan, R.; Sarangapani, S.; Smotkin, E. S.; Mallouk, T. E. *Science* **1998**, *280*, 1735−1737.
(13) Xiang, X. D.; Su, X.; Briceno, G.; Lou, Y.; Wang, K. A.; Chang, H.; Freedman, W. G. W.; Chen, S. W.; Schultz, P. G. *Science* **1995**, *268*, 1738−1740.
(14) Potyrailo, R. A.; Chisholm, B. J.; Morris, W. G.; Cawse, J. N.; Flanagan, W. P.; Hassib, L.; Molaison, C. A.; Ezbiansky, K.; Medford. G.; Reitz, H. *J. Comb. Chem*. **2003**, *5*, 472−478.
(15) Potyrailo, R. A.; Chisholm, B. J.; Olson, D. R.; Brennan, M. J.; Molaison, C. A. *Anal. Chem*. **2002**, *74*, 5105−5111.
(16) Potyrailo, R. A.; Olson, D. R.; Medford, G.; Brennan, M. J. *Anal. Chem*. **2002**, *74*, 5676−5680.
(17) Beattie, S. D.; Dahn, J. R. *J. Electrochem. Soc*. **2003**, *150*, C457−C460.
(18) Baeck, S. H.; Jaramillo, T. F.; Brandli, C.; McFarland, E. W. *J. Comb. Chem*. **2002**, *4*, 563−568.
(19) Siu, T.; Yekta, S.; Yudin, A. K. *J. Am. Chem. Soc*. **2000**, *122*, 11787−11790.
(20) Simon, U.; Sanders D.; Jockel, J.; Heppel, C.; Brinz, T. *J. Comb. Chem*. **2002**, *4*, 511−515.
(21) Brandli, C.; Jaramillo, T. F.; Ivanovskara, A.; McFarland, E. W. *Electrochim. Acta* **2001**, *47*, 553−557.
(22) Sullivan, M. G.; Utomo, H.; Fagan, J. P.; Ward, M. D. *Anal. Chem*. **1999**, *71*, 4369−4375.
(23) Sun, Y. P.; Buck, H.; Mallouk, T. E. *Anal. Chem*. **2001**, *73*, 1599−1604.
(24) Spong, A. D.; Vitins, G.; Guerin, S.; Hayden, B. E.; Russell, A. E.; Owen, J. R. *J. Power Sources* **2003**, *119*, 778−783.
(25) Jambunathan K.; Hillier A. C. *J. Electrochem. Soc*. **2003**, *150*, E321−E320.
(26) Fernadez, J. L.; Bard, A. J. *Anal. Chem*. **2003**, *75*, 2976−2974.
(27) Jiang, R. Z.; Chu, D. *J. Electroanal. Chem*. **2002**, *527*, 137−142.
(28) Choi, W. C.; Kim, J. D.; Woo, S. I. *Catal. Today* **2002**, *74*, 235−240.
(29) Jayaraman, S.; Hillier, A. C. *J. Phys. Chem. B* **2002**, *107*, 5221−5230.
(30) Chu, Y. H.; Shul, Y. G.; Choi, W. C.; Woo, S. I.; Han, H. S. *J. Power Sources* **2003**, *118*, 334−341.
(31) Liu, R. X.; Smotkin E. S. *J. Electroanal. Chem*. **2002**, *535*, 49−55.
(32) Gurau, B.; Viswanathan, R.; Liu, R. X.; Lafrenz, T. J.; Ley, K. L.; Smotkin, E. S.; Reddington, E.; Sapienza, A.; Chan, B. C.; Mallouk, T. E.; Sarangapani, S. *J. Phys. Chem. B* **1998**, *102*, 9997−10003.
(33) Chen, G. Y.; Delafuente, D. A.; Sarangapani, S. Mallouk, T. E. *Catal. Today* **2001**, *67*, 341−355.
(34) Ren, X. M.; Springer, T. E.; Zawodzinski, T. A..; Gottesfeld, S. *J. Electrochem. Soc*. **2000**, *147*, 466−474.
(35) Jiang, R. Z.; Chu, D. *Electrochem. Solid-State Lett*. **2002**, *5*, A156−A159.
(36) Kim, J.; Lee, S. M.; Srinivasan, S.; Chamberlin, C. E. *J. Electrochem. Soc*. **1995**, *142*, 2670−2674.
(37) Rho, Y. W.; Velev, O. A.; Srinivasan, S.; Kho Y. T. *J. Electrochem. Soc*. **1994**, *141*, 2084−2088.

CC0498581